Differential expression of genes associated with hypoxia pathway on bone marrow stem cells in osteoporosis patients with different bone mass index

Qi Zhu[1,2#], Chang Shan[1,3#], Ling Li[1], Lige Song[1], Keqin Zhang[1], Yun Zhou[1]

[1]The Endocrinology Department of Shanghai Tongji Hospital, Tongji University School of Medicine, Shanghai 200065, China; [2]The Geriatric Department of Shanghai General Hospital, Shanghai Jiaotong University, Shanghai 200080, China; [3]Department of Endocrine and Metabolic Diseases, Rui-Jin Hospital, Shanghai Jiao Tong University School of Medicine, Shanghai Clinical Center for Endocrine and Metabolic Diseases, Shanghai Institute of Endocrine and Metabolic Diseases, Shanghai 200025, China

Contributions: (I) Conception and design: Q Zhu, C Shan, Y Zhou; (II) Administrative support: Y Zhou; (III) Provision of study materials or patients: Q Zhu, C Shan, L Li, L Song, K Zhang; (IV) Collection and assembly of data: Q Zhu, C Shan, L Li, L Song, K Zhang; (V) Data analysis and interpretation: Q Zhu, C Shan; (VI) Manuscript writing: All authors; (VII) Final approval of manuscript: All authors.

[#]These authors contributed equally to this work.

Correspondence to: Yun Zhou; Keqin Zhang. Department of Endocrinology, Shanghai Tongji Hospital, Tongji University School of Medicine, Shanghai 200065, China. Email: zhouyunsy@126.com; 13621798084@126.com.

Background: This study aimed to assess gene expression changes associated with hypoxia pathway on bone marrow stem cells (BMSCs) and explore effects of bone mass index (BMI) on hypoxia pathway of osteoporosis (OP) patients.

Methods: Human BMSCs were isolated from bone marrow. Subjects were divided into healthy control group and OP group which was further divided into BMI <25 OP subgroup and BMI ≥25 OP subgroup.

Results: The genes downregulated in OP patients were involved in hypoxia pathway. Furthermore, those genes were even downregulated in OP patients BMI ≥25 subgroup than OP patients BMI <25 subgroup. The genes were expressed in response to decreased oxygen levels, and their functions are related to photoperiodism, positive regulation of myoblast differentiation, and entrainment of circadian clock by gene ontology (GO) analysis.

Conclusions: The expression of genes associated with hypoxia pathway on BMSCs in OP patients are lower than healthy subjects, and the expression of genes related to carbohydrate metabolism are lower in overweight OP patients than in normal weight OP patients. These results need further research.

Keywords: Bone marrow stem cells (BMSCs); osteoporosis (OP); hypoxia pathway; bone mass index (BMI)

Introduction

Aging bone loss and osteoporosis (OP) are characterized by decreased bone mass which is caused by the disruption of the balance between bone formation and bone resorption. Studies showed that decreased bone formation was partially caused by bone marrow mesenchymal stem cells (BMSCs), a common precursor of osteoblasts and bone marrow adipocytes, which inclined to differentiate into adipocytes and caused increased marrow fat. Many factors would affect the BMSC differentiation in bone marrow cavity (1), among which hypoxia inducible factor (HIF), a member of Helix-loop-helix family, is a pivotal one and plays a key role in BMSC differentiation.

The bone marrow cavity is one of the most hypoxic microenvironment of human body. Low oxygen level within the bone marrow would promote hypoxia signaling pathways

Page 2 of 14

Zhu et al. Genes in hypoxia pathway on BMSC in OP

such as HIF, which is regulated by oxygen requiring prolyl hydroxylases (PHDs) and von Hippel-Lindau (VHL) tumor suppressor (2). These hypoxia signaling pathways have profound effects on bone development and homeostasis (3). It is well-known that bone marrow is desaturated and contains oxygen concentration ranging from 1% to 7% despite its high degree of vascularization (4). The levels of O_2 consumption by leukocytes as well as blood speed in the sinusoids were contributed to the generation of a gradient of oxygenation (2). Healthy bone marrow can provide balanced hypoxic microenvironments. It has been confirmed by direct measurements of PO_2 in the bone marrow of mice that hypoxic conditions existed in perivascular areas even at a 5-cell distance from a blood sinus (5).

Dong-Feng *et al.* (6) found that down-regulated the expression of HIF1α could reduce the adhesion and secretion function of hBMSC in acute leukemia, which indicates that hypoxia signaling pathway plays an important role in regulating hBMSC function (7). Furthermore, with aging, oxidative stress and inflammation occurred, adipocyte differentiation increased in bone marrow with a disruption of hypoxic osteoblastic niches (8). And it remains unclear whether adipocytes respond to the same bone marrow microenvironment in a possibly opposite manner in regulating BMSC proliferation and differentiation. HIF and its target genes from hBMCSs were found up-regulated in patients with psoriasis (9), which may be caused by aberrant immunoregulatory and chemotactic function of BMSCs. HIF also can be mediated by inflammation (10). OP was reported to related to inflammation and immunity (11,12), thus BMSCs function was investigated from OP patients. Consequently, it is logical to study hypoxia pathway gene expression on the BMSCs from OP patients.

Besides, obesity is a potent risk factor for metabolic diseases at the population level. At the individual patient level, however, correlations between body mass index and bone mineral density are not always straightforward due, in part, to differences among adipose tissue depots with respect to the overall rate of adipocyte dysfunction, local degree of inflammation, and tissue vascularization (13). Hypoxia has been proposed as a key underlying mechanism triggering tissue dysfunction (14). The root cause of obesity-related adipose tissue dysfunction is viewed as oxygen deficiency or "hypoxia", pushing the tissue toward a proinflammatory environment (15,16). It remains unclear whether obesity could further influence hypoxic pathway gene expression on BMSCs of OP patients.

In this study, the Qiagen Human Hypoxia Signaling Pathway PCR Array was firstly used to screen for differently expressed genes associated with hypoxia pathway on hBMSCs between normal controls and OP patients which were further divided into bone mass index (BMI) <25 OP subgroup and BMI ≥25 OP subgroup separately. Based on information above, Real-time PCR, western blot and immunohistochemistry were further performed to verify the expression level of certain hypoxia genes on BMSCs of OVX-induced OP mice model. The aim of this study was to compare the expression of hypoxia pathway genes between normal controls and OP patients of different BMI and provide a view of the potential regulation of hypoxia signaling pathway on OP bone marrow microenvironment and bone metabolism.

Methods

Participants

This study was approved by the Ethics Committee of Shanghai Tongji Hospital (KYSB-2015-20). A total of 6 patients with OP (marked decline in BMD, spine T-score ≤−2.5) and 3 control subjects were recruited from Endocrinology Department of Shanghai Tongji Hospital between March 2014 and June 2014. Patients with OP were further divided into 2 subgroups according to their BMI: BMI <25 (n=3) and BMI ≥25 (n=3). Informed consent was provided by all participants.

All participants were questioned of their medication history and verified no serious complications existed such as cancer, cardio-pulmonary diseases and all diseases that may cause secondary OP. Totally, 6 patients with OP participated in this study prior to the start of any treatment. Both the spine and femoral neck T-score was measured for each participant. T-scores of spine (L1-L4) and femoral neck were obtained by using a dual energy X-ray absorptiometry scanner (Lunar DXA, USA). The hBMSCs from anterior superior iliac crest of all participants were investigated in this study.

Isolation hBMSCs from human anterior superior iliac crest

Fresh human bone marrow was harvested from the anterior superior iliac crest of 6 patients and 3 volunteers during bone marrow biopsy (Shanghai Tongji Hospital, Shanghai, China). Patients were provided informed consent using guidelines approved by the Shanghai Tongji Hospital. From

bone marrow aspirates, the mononuclear cell fraction was harvested for MSC isolation using conventional density gradient centrifugation with a density gradient solution (Ficoll-Paque PREMIUM, Sigma-Aldrich, MO, USA). The resulting cells were collected and isolated (17).

Microarray analysis

To analyze the genes expression changes associated with hypoxia pathway on BMSCs, the PAHS-032Z Human Hypoxia Signaling Pathway PCR Arrary (Qiagen) was used. All the gene information was described in *Table S1*.

OP mice model

Thirty 8-week-old C57 female mice were randomly equally divided into SHAM group and OVX group. All the mice were housed under 12 h light/12 h dark cycles, temperature 20.0±2.0 ℃ and relative humidity of 55%±10%. Food and water were available ad libitum. All procedures were performed according to the National Institutes of Health for the care and use of laboratory animals (NIH publication No 80-23) and were approved by the Animal Ethics Committee of Shanghai Tongji Hospital. Despite that OVX group mice received complete resection on both sides of ovarian while equal amount of fat was resected in SHAM group, other procedures were all the same. All the mice were killed 12 weeks after surgery and both sides of femur and tibia were separated under aseptic condition. Right femur and tibia were used to get original mBMSCs; left femur was used for immunohistochemical staining.

Cell culture

mBMSCs were isolated according to the following method. In brief, femurs and tibias from mice were removed. Muscle and extraossial tissue were trimmed. The ends of bones were cut and the marrow was flushed using a needle and syringe. The whole BM cells were cultured in α-MEM (Gibco) supplemented with 10% FBS and penicillin (100 U/mL)/ streptomycin (100 µg/mL) at 37 ℃ in humid air with 5% CO_2 and then nonadherent cells were removed thoroughly 24 h later. Afterwards, replace the cell medium every 48 h to remove non-adherent cells to get purified mBMSCs.

RNA preparation and quantitative real-time PCR

Total RNA was isolated using TriZol (Invitrogen, CA,

USA) and purified from cell pellet using RNeasy mini kit as recommended by the manufacturer (Qiagen). Using the Primescript RT Reagent kit (Takara, Japan), 1 µL of total RNA was reverse-transcribed into 20 µL cDNA. Quantitative Real-time PCR was performed in a 10 µL reaction mixture in ABI Prism 7900HT system (Applied Biosystems, CA, USA) using SYBR Premix Ex TaqTM II (Takara, Japan) according to the manufacturer's instructions. The 10 µL PCR reaction mixture contained 5 µL SYBR, 0.4 µL primer, 0.2 µL ROX, 3.4 µL ddH2O and 1 µL cDNA. The primers used were presented in the following: 5'-CAGCCTTCCTTCTTGGGTAT-3' and 3'-GGCATAGAGGTCTTTACGG-5' for β-actin; 5'-GAAAGGATCGGCGCAATTAA-3' and 3'-CATCATCCGAAAGCTGCATC-5' for BHLHE40; 5'-CGAGCATGACGAAGAGATCAT-3' and 3'-TCGAAGGTTGGCCTATCTGA-5' for PIM1.

Western blot

Protein lysates of mBMSC were separated using 8% SDS-PAGE gel electrophoresis and then transferred to PVDF membrane and blocked with 5% BSA. The primary antibodies for β-actin (1:1,000, Abcam) and Bhlhe40 (1:50, Genetex, CA, USA) were incubated on shaking bed overnight at 4 ℃. Secondary antibody was incubated at room temperature for 1 h. Developed films were digitized by scanning and the optical densities were analyzed by AlphaView SA software (V3.3.0, Cell Biosciences).

Histology

Tibias were removed and fixed in PLP fixative (2% paraformaldehyde containing 0.075 M lysine and 0.01 M sodium periodate) overnight at 4 ℃ and processed histologically as described (18). Tibias were decalcified in ethylene diamine tetraacetic acid (EDTA)-glycerol solution for 5 to 7 days at 4 ℃. Decalcified tibias were dehydrated and embedded in paraffin, after which 5 mm sections were cut on a rotary microtome (RM2235, Leica, Germany). These sections were stained with hematoxylin and eosin (HE) or histochemically for total collagen or immunohistochemical staining as described in the next section.

Immunohistochemical staining

Immunohistochemical staining for Bhlhe40 was performed using the avidin-biotin-peroxidase complex technique with

Page 4 of 14

Zhu et al. Genes in hypoxia pathway on BMSC in OP

Table 1 Demographic characteristics of participants

Item	Healthy control (n=3)	Osteoporosis		
		BMI <25 (n=3)	BMI ≥25 (n=3)	P value
Age (years)	52.67±1.15	59±3.61	52.67±5.86	0.186
BMI (kg/m^2)	20.91±1.62	19.8±3.87	26.37±0.90	0.046
HbA1c (%)	4.97±0.55	5.07±0.21	6.27±1.25	0.176
TC (mmol/L)	2.24±1.91	4.37±0.78	4.92±1.20	0.591
TG (mmol/L)	2.26±1.40	1.99±1.52	2.62±1.09	0.544
ALT (U/L)	16±4.58	16.67±2.52	22.33±9.50	0.374
AST (U/L)	13.67±2.30	17.67±3.51	17.67±6.66	1.000
HB (g/L)	158.67±15.70	126.33±9.87	127.67±17.04	0.912
Cr (μmol/L)	86±9.85	63.33±3.51	68.33±28.57	0.779

Data are expressed as the mean ± SD. There was no significant difference between osteoporosis subgroups except BMI. No significant differences existed between healthy control group and osteoporosis group (data are not shown). BMI, body mass index.

primary antibody rabbit polyclonal anti-Bhlhe40 (1:50, Genetex, CA, USA). Briefly, endogenous peroxidase was blocked with 3% H_2O_2 and sections were treated overnight at 4 ℃ with primary antibodies. Sections were then incubated with the secondary antibody (KIT-5010, Max Version, Maixin.Bio, China) for 1 h at room temperature, followed by coloration with 3,3-diaminobenzidine (DAB, Sigma, Germany) and hematoxylin counterstaining. The sections were washed with 0.01 mol/L PBS between each step.

Data analysis

Calculate the ΔCt for each pathway-focused gene in each treatment group.

ΔCt (group 1) = average Ct – average of HK genes' Ct for group 1 array;

ΔCt (group 2) = average Ct – average of HK genes' Ct for group 2 array.

Calculate the ΔΔCt for each gene across two PCR arrays (or groups).

ΔΔCt = ΔCt (group 2) – ΔCt (group 1).

Where group 1 is the control and group 2 is the experimental.

Calculate the fold-change for each gene from group 1 to group 2 as 2-ΔΔCt.

If the fold-change is greater than 1, then the result may be reported as a fold up-regulation. If the fold-change is less than 1, then the negative inverse of the result may be

reported as a fold down-regulation. Statistical analyses also were performed and P value correction to account for a high false-positive rate was performed by using the false discovery rate method.

Statistical analysis

Measurement data were expressed as mean ± standard deviation (SD). Significance of the difference between two groups was analyzed using two-tailed Student's *t*-test. All statistical analyses were performed with SPSS 20.0 software (IBM, Armonk, NY, USA). P<0.05 was considered statistically significant. Statistical analyses were performed and P value correction to account for a high false-positive rate was performed by using the false discovery rate method with the R package limma in Bioconductor. Volcano Plot and GO analysis of differentially expressed mRNAs and between group statistical analysis were performed.

Results

Demographic characteristics of participants

The demographic characteristics of the participants are summarized (*Table 1*).

One female and 5 males with OP were investigated in this study. Mean age of 6 patients was 55 years. Healthy controls were comprised of 3 healthy males with a normal BMD (*Table 2*). Except BMD, no significant differences existed between healthy control group and OP group (data

Table 2 BMD of participants recruited for the study

BMD	Healthy control (n=3)	Osteoporosis (n=6)	P value
L1 BMD (g/cm^3)	0.91±0.02	0.63±0.06	0.000125
L2 BMD (g/cm^3)	0.96±0.04	0.68±0.09	0.001876
L3 BMD (g/cm^3)	1.00±0.08	0.70±0.07	0.000717
L4 BMD (g/cm^3)	1.00±0.08	0.71±0.07	0.001377
Total BMD (g/cm^3)	0.97±0.06	0.69±0.07	0.000462
Neck BMD (g/cm^3)	0.84±0.05	0.60±0.08	0.003156
T score	−0.8±0.15	−3.33±0.51	–

Data are expressed as the mean ± SD. BMD was significantly decreased in osteoporosis group compared with healthy control group.

Table 3 BMD of osteoporosis subgroups recruited for the study

BMD	Osteoporosis		P value
	BMI <25 (n=3)	BMI ≥25 (n=3)	
L1 BMD (g/cm^3)	0.63±0.06	0.65±0.08	0.553
L2 BMD (g/cm^3)	0.68±0.09	0.73±0.09	0.211
L3 BMD (g/cm^3)	0.70±0.07	0.72±0.10	0.610
L4 BMD (g/cm^3)	0.72±0.08	0.71±0.09	0.960
Total BMD (g/cm^3)	0.69±0.07	0.71±0.09	0.071
Neck BMD (g/cm^3)	0.60±0.08	0.67±0.08	0.071
T score	−3.23±0.5	−3.43±0.50	–

Data are expressed as the mean ± SD. No significant differences existed between osteoporosis subgroups. BMI, body mass index.

are not shown). These results do not change much when the data were removed from the female patients. The OP patients can be further divided into two subgroups according to their BMI, except which no other significant differences existed between these two subgroups (*Table 3*).

Normoxic downregulation of hypoxia related genes from hBMSCs in OP patients

Among the hypoxia signaling pathway genes, the expression levels of 7 genes (BHLHE40, HIF1AN, MAP3K1, MET, PER1, IL1B, PFKFB3 and PIM1) were down-regulated when compared with control group. Particularly, PER1 was significantly down-regulated. No gene expression was found be up-regulated in OP group compared with control group (*Table 4*). Some important downregulated GO functions may be related to response to decreased oxygen levels, photoperiodism, positive regulation of myoblast differentiation and entrainment of circadian clock by photoperiod (*Figure 1*).

Screening for differential genes from BMI <25 OP subgroup and control group

Among the hypoxia signaling pathway genes, the expression levels of 8 genes (*ADM*, *BHLHE40*, *MAP3K1*, *LOX*, *TXNIP*, *NAMPT*, *PFKFB3* and *PIM1*) were down-regulated in BMI <25 OP subgroup when compared with the control group. Particularly, NAMPT was significantly down-regulated. Two genes (*ANGPTL4*, *SLC16A3*) expression were found to be up-regulated in BMI <25 OP subgroup compared with control group (*Table 5*).

Screening for differential genes from BMI ≥25 OP subgroup and control group

Among the hypoxia signaling pathway genes, the expression levels of 15 genes (*ANXA2*, *BHLHE40*, *DDIT4*, *DNAJC5*,

Page 6 of 14

Zhu et al. Genes in hypoxia pathway on BMSC in OP

Table 4 Differential genes from osteoporosis group and control group

Gene symbol	Fold up-/down-regulation, osteoporosis/control	t-test, P value	FDR, Q value
BHLHE40	−2.85	0.001576	0.04727
HIF1AN	−2.52	0.010969	0.06581
MAP3K1	−3.69	0.003010	0.04963
MET	−4.28	0.038899	0.12964
PER1	−6.39	0.004551	0.05461
PFKFB3	−3.76	0.000486	0.02918
PIM1	−5.33	0.001885	0.03769
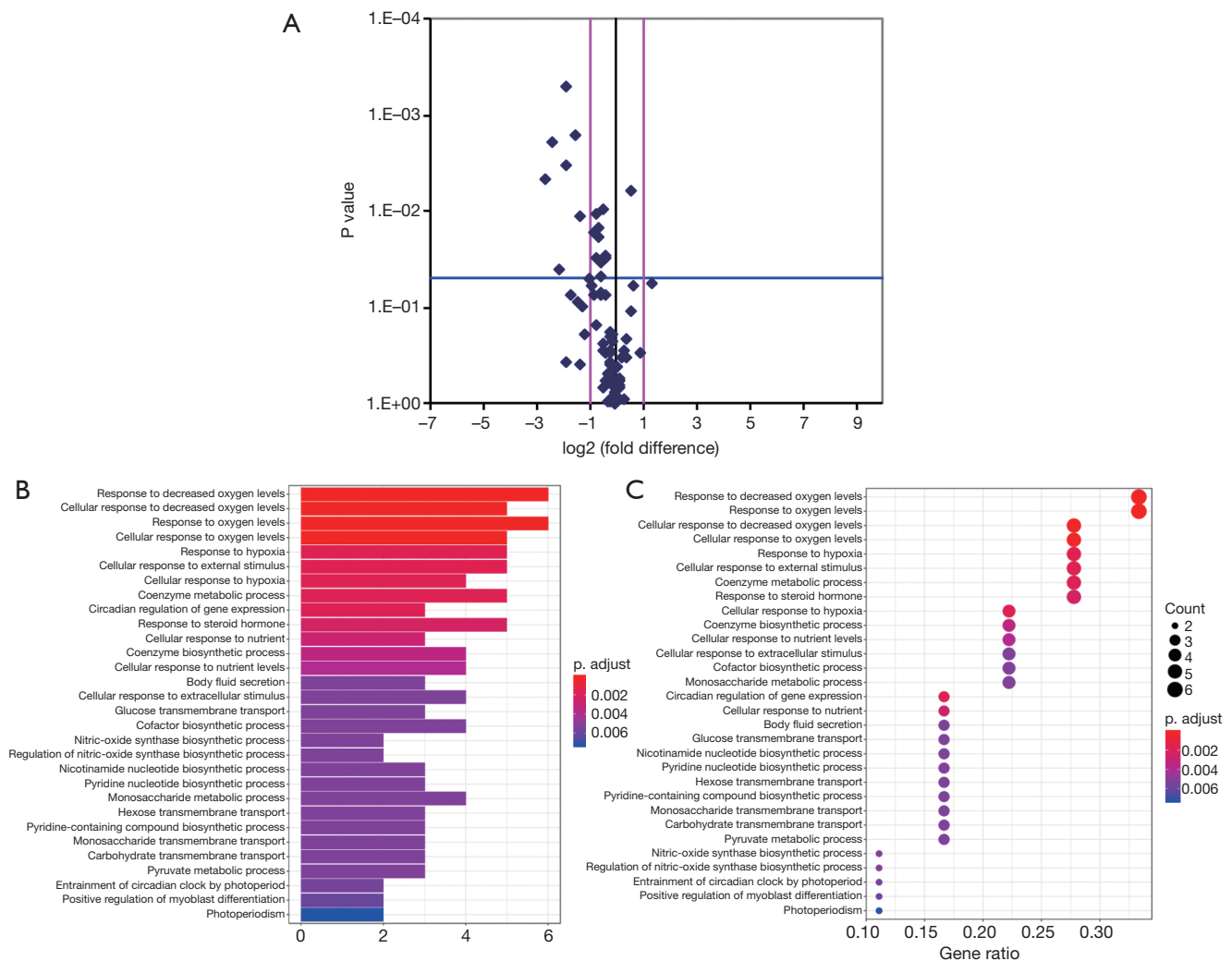
Figure 1 Volcano plot of significantly differential experiment genes and significant gene ontology (GO) analyses and pathways of differentially expressed genes. (A) Analyzing the differentially expressed genes by t-test, log2 (fold change) was taken as abscissa and negative logarithm-log10 (P value) of P value was taken as ordinate. (B) The significant GO of differentially expressed genes. (C) The significant function of differentially expressed genes. The y axis shows the GO or pathway category and the x axis shows the negative logarithm of the P value (–LgP). A larger –LgP indicated a smaller P value for the difference.

Table 5 Differential genes from BMI <25 osteoporosis subgroup and control group

Gene symbol	Fold up-/down-regulation, osteoporosis/control	t-test, P value	FDR, Q value
ADM	−2.14	0.011382	0.08473
BHLHE40	−2.19	0.029789	0.09504
LOX	−2.20	0.037472	0.10916
MAP3K1	−2.04	0.022416	0.08348
NAMPT	−4.66	0.001422	0.04765
PFKFB3	−2.53	0.011585	0.07762
PIM1	−3.16	0.036125	0.11001
TXNIP	−2.12	0.012865	0.07836
SLC16A3	5.26	0.006528	0.08748
ANGPTL4	3.36	0.023373	0.08700

BMI, body mass index.

GYS1, *HIF1AN*, *MAP3K1*, *P4HB*, *PER1*, *PFKFB3*, *PFKL*, *PIM1*, *SLC2A1*, *TP53* and *USF2*) were down-regulated in BMI ≥25 OP subgroup when compared with the control group. Particularly, PFKL was significantly down-regulated. No gene expression was found be up-regulated in BMI ≥25 OP subgroup compared with control group (*Table 6*).

Screening for differential genes from BMI <25 OP subgroup and BMI ≥25 OP subgroup

Among the hypoxia signaling pathway genes, the expression levels of 12 genes (*ANXA2*, CA9, *DDIT4*, GYS1, *MAP3K1*, *P4HB*, *PFKFB3*, *PFKL*, *PGF*, *SLC16A3*, *SLC2A1* and *TP53*) were down-regulated in BMI ≥25 OP subgroup when compared with the BMI <25 OP subgroup. Particularly, PFKL and SLC16A3 were significantly down-regulated. Two genes (*NAMPT*, *NCOA1*) expression were found to be up-regulated in BMI ≥25 OP subgroup compared with BMI <25 OP subgroup (*Table 7*). Some important downregulated GO functions may be related to metabolic and glycolytic genes (*Figure 2*).

Expression of hypoxia pathway genes on mBMSCs

Based on previous microarray screening on differently expressed hypoxia signaling pathway genes between OP patients and normal controls, real-time PCR and Western blot were performed to verify the expression level of certain hypoxia genes on mBMSCs of OVX and SHAM mice model. Compared with mBMSCs of SHAM mice,

the expression of PIM1 on mRNA level (*Figure 3A*) and the expression of BHLHE40 on both mRNA (*Figure 3B*) and protein level (*Figure 3C*) decreased significantly on mBMSCs of OVX mice, which was consistent with the results of previous microarray screening.

Evaluation of mice model and expression of BHLHE40 in femur bone marrow of mouse model

Morphologic and histological analyses of proximal femora were performed with HE staining and histochemistry for total collagen (*Figures 4* and *5*). Compared with SHAM mice, the number, thickness and length of trabecular bone (*Figure 4A,B*) and the expression of total collagen (*Figure 4D,E*) in OVX mice decreased significantly with significantly increased number of adipocytes in bone marrow (*Figure 4C*), which indicated the OVX mice models were successfully built.

The BHLHE40 expression was analyzed by immunohistochemistry in this study. It showed that the BHLHE40 expression of OVX mice decreased markedly compared with that of the SHAM group (*Figure 5*).

Discussion

Hypoxia is a critical factor for stem cells in bone marrow by protecting them from ROS-mediated damage, which allows them to maintain normal function and self-renewal potential. The roles of hypoxia in the differentiation of MSCs remain controversial. MSCs under reduced oxygen

Page 8 of 14

Zhu et al. Genes in hypoxia pathway on BMSC in OP

Table 6 Differential genes from BMI ≥25 osteoporosis subgroup and control group

Gene symbol	Fold up-/down-regulation, osteoporosis/control	*t*-test, P value	FDR, Q value
ANXA2	−3.27	0.010590	0.05703
BHLHE40	−3.73	0.009262	0.05403
DDIT4	−8.55	0.028992	0.10681
DNAJC5	−2.54	0.017724	0.07298
GYS1	−7.48	0.007312	0.05119
HIF1AN	−3.40	0.017200	0.07525
MAP3K1	−6.70	0.000017	0.08717
P4HB	−2.64	0.006077	0.06077
PER1	−8.20	0.035503	0.01183
PFKFB3	−5.59	0.001887	0.04402
PFKL	−16.04	0.000010	0.08109
PIM1	−8.99	0.006255	0.05473
SLC2A1	−4.92	0.004637	0.08114
TP53	−6.38	0.006409	0.04984
USF2	−2.13	0.016859	0.07867

BMI, body mass index.

Table 7 Differential genes from BMI <25 osteoporosis subgroup and BMI ≥25 osteoporosis subgroup

Gene symbol	Fold up-/down-regulation, BMI ≥25/BMI <25	*t*-test, P value	FDR, Q value
ANXA2	−2.64	0.002236	0.03131
CA9	−4.20	0.038368	0.16786
DDIT4	−6.66	0.001337	0.03119
GYS1	−8.61	0.009239	0.07186
MAP3K1	−3.29	0.047246	0.19454
P4HB	−2.38	0.037994	0.18997
PFKFB3	−2.21	0.038362	0.17902
PFKL	−19.15	0.000013	0.00091
PGF	−2.07	0.021402	0.14982
SLC16A3	−25.84	0.001075	0.03763
SLC2A1	−4.76	0.006630	0.06630
TP53	−5.31	0.004376	0.05106
NAMPT	3.75	0.027735	0.16179
NCOA1	2.14	0.027111	0.17253

BMI, body mass index.
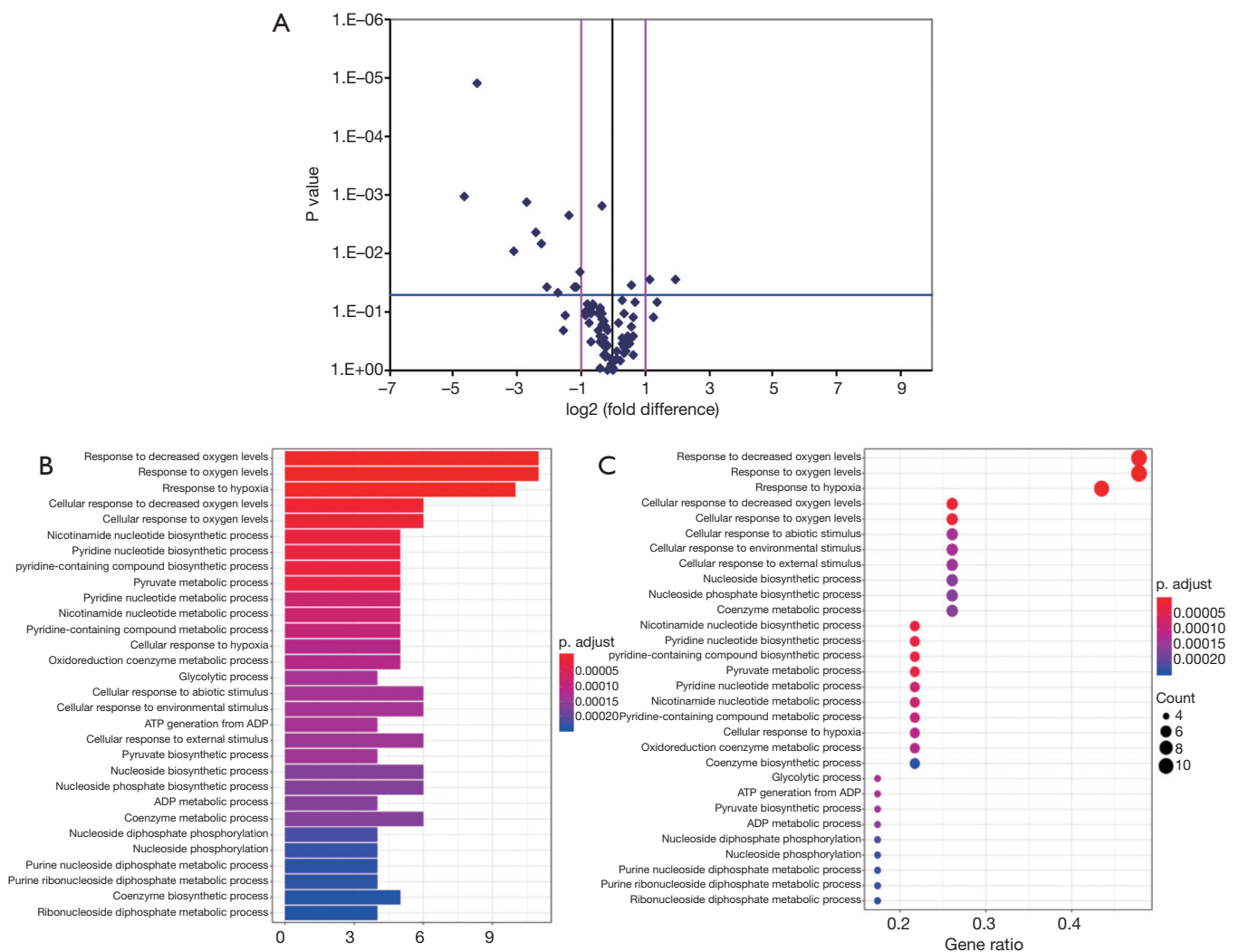
Figure 2 Volcano plot of significantly differential experiment genes and significant gene ontology (GO) analyses and pathways of differentially expressed genes. (A) Analyzing the differentially expressed genes by *t*-test, log2 (fold change) was taken as abscissa and negative logarithm-log10 (P value) of P value was taken as ordinate. (B) The significant GO of differentially expressed genes. (C) The significant function of differentially expressed genes. The y axis shows the GO or pathway category and the x axis shows the negative logarithm of the P value (–LgP). A larger –LgP indicated a smaller P value for the difference.

conditions were believed to preserve their stemness and remain undifferentiated (19). However, it was also reported that hypoxia enhances mesoderm lineage differentiation, including adipogenic, osteogenic or chondrogenic differentiation (20,21). Studies comparing fracture incidence in obese and non-obese individuals have demonstrated that obesity, defined on the basis of body mass index (BMI), is associated with increased risk of fracture at some sites but seems to be protective at others (22). Extensive research using genetic models has revealed that hypoxia signaling is

a key mechanism in adipose tissue dysfunction, leading to adipose tissue fibrosis, inflammation and insulin resistance (23,24). Consequently, it is quite significant to study hypoxia pathway gene expression on the BMSCs from OP patients, furthermore, whether the adipose tissue exert effect on hBMSC function.

Data in this study indicated that hypoxic pathway genes were down-regulated in the BMSCs from OP patients. Genes were found down-regulated when compared with the control group. Some important downregulated GO

Page 10 of 14

Zhu et al. Genes in hypoxia pathway on BMSC in OP
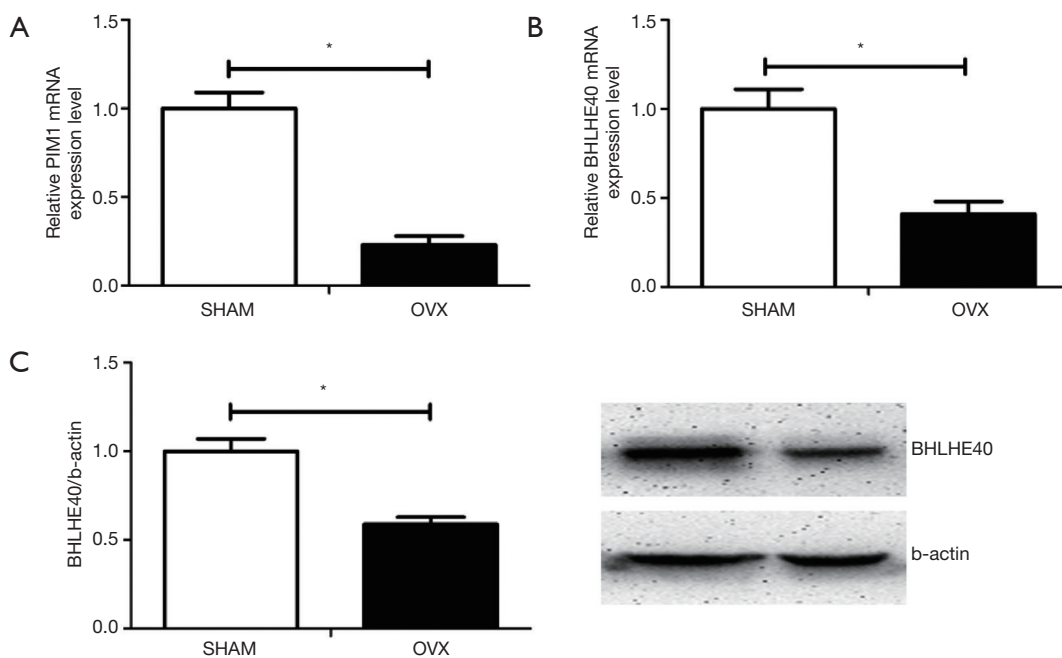
Figure 3 Expression of BHLHE40 and PIM1 on mBMSCs of mice model. (A) Relative expression of PIM1 on mRNA level; (B) relative expression of BHLHE40 on mRNA level; (C) relative expression of Bhlhe40 on protein level. All experiments in this figure were repeated at least three times, and data were expressed as mean ± SD. *, P<0.05 compared with SHAM group.
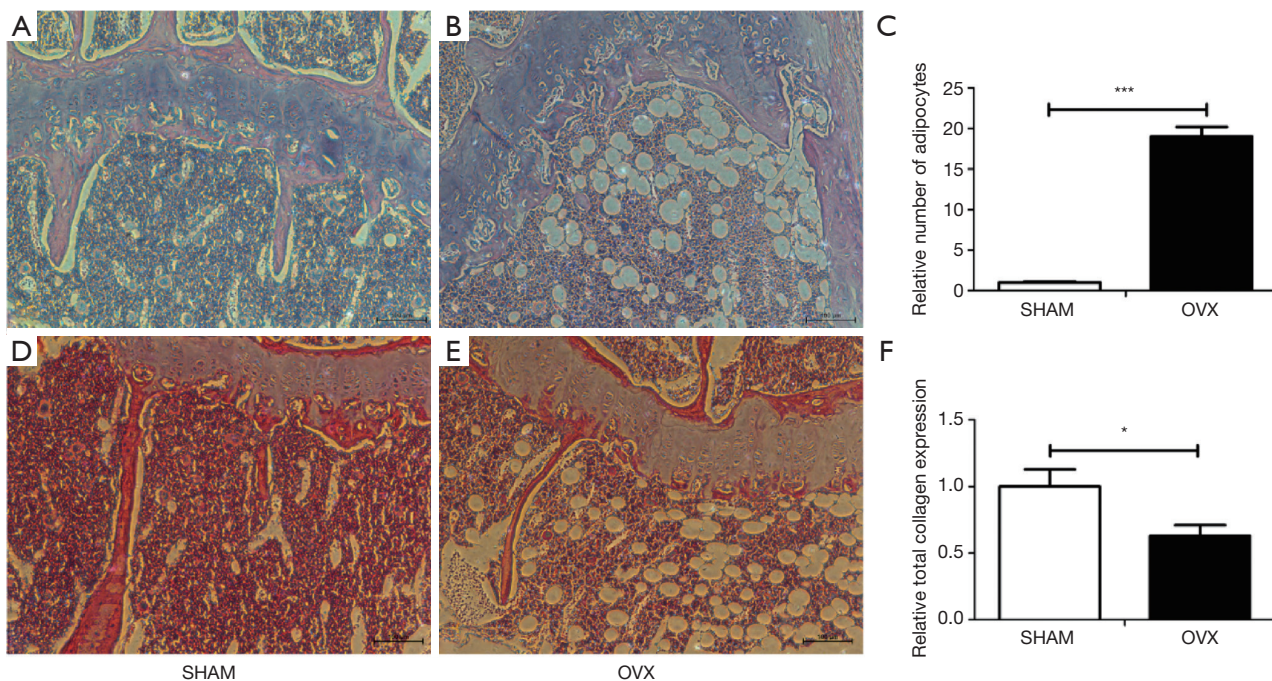
Figure 4 Evaluation of mice model by HE staining and histochemistry for total collagen. (A,D) HE staining and total collagen expression of SHAM mice (10×10); (B,E) HE staining and total collagen expression of OVX mice (10×10); (C) relative number of adipocytes in bone marrow of SHAM and OVX mice; (F) relative total collagen expression of SHAM and OVX mice. All experiments in this figure were repeated at least three times, and data were expressed as mean ± SD. *, P<0.05; ***, P<0.001 compared with SHAM group.
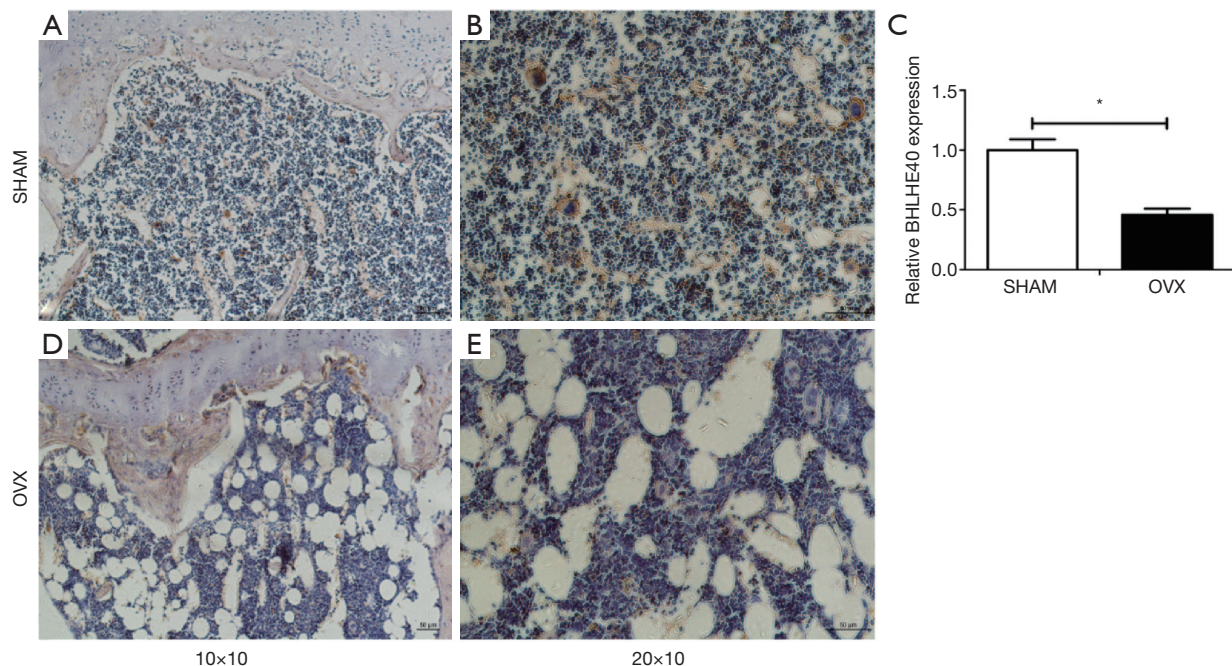
Figure 5 Expression of Bhlhe40 of SHAM and OVX mice by immunohistochemistry. (A) Expression of Bhlhe40 of SHAM mice (10×10); (B) expression of Bhlhe40 of SHAM mice (20×10); (D) expression of Bhlhe40 of OVX mice (10×10); (E) expression of Bhlhe40 of OVX mice (20×10); (C) relative expression of Bhlhe40 between two groups. All experiments in this figure were repeated at least three times, and data were expressed as mean ± SD. *, P<0.05 compared with SHAM group.

functions may be related to photoperiodism, positive regulation of myoblast differentiation and entrainment of circadian clock by photoperiod, among which PER1 was significantly down-regulated. PER1 encodes the period circadian protein homolog 1 protein in human and studies have demonstrated that the PER1 polymorphisms were singly and in combination related to the lumbar spine BMD (25). These data further explained the potential important function of PER1 on hypoxia pathway and OP. Basic helix-loop-helix transcription factor BHLHE40 (DEC1) promotes chondrogenic differentiation of MSC and myoblast differentiation in early and terminal stage and modulated the osteogenic differentiation of MSC (26,27). Disruption of hypoxic microenvironment in bone marrow of OP patients causes decreased DEC1 expression, which might affect the differentiation of BMSCs, further leading to decreased bone formation. Thus, DEC1 may play an important role in both hypoxia pathway and OP, but further studies are still needed. The serine/threonine kinase Pim1 is an important regulator of cell proliferation and survival, cell metabolism and transcriptional activity (28), which has not been studied in OP yet. Besides, studies have demonstrated

its importance in anti-proinflammation (18). This study may shed new light on the important function of PIM1 in OP. PIM1 and BHLHE40 expression was further checked in mice OP model, which also down-regulated than control group.

This study further confirmed the expression of PIM1 and BHLHE40 decreased significantly on mBMSCs of OVX mice, which was consistent with the results of previous microarray screening in human BMSCs. Basic helix-loop-helix transcription factor BHLHE40 (DEC1) promotes chondrogenic differentiation of MSC in early and terminal stage and modulated the osteogenic differentiation of MSC (26). Disruption of hypoxic microenvironment in bone marrow of OP patients causes decreased DEC1 expression, which might affect the differentiation of BMSCs, further leading to decreased bone formation. Thus, DEC1 may play an important role in both hypoxia pathway and OP, but further studies are still needed. The serine/threonine kinase Pim1 is an important regulator of cell proliferation and survival, cell metabolism, and transcriptional activity (28), which has not been studied in OP yet. Besides, studies have demonstrated its importance in anti-proinflammation (18).

Page 12 of 14

Zhu et al. Genes in hypoxia pathway on BMSC in OP

This study may shed new light on the important function of PIM1 in OP.

Transcription factor HIF-1 has been reported to play a major role in the induction of hypoxia-inducible genes including many glycolytic enzymes, VEGF, and erythropoietin (29). However, in this study, it was found that HIF-1 expression was down-regulated without statistical significance (data were not shown) while HIF-1 inhibitor FIH was down-regulated dramatically. This may partly attribute to unstable expression of HIF-1 under the normoxia environment and the limitation by the sample size as the genes downstream of HIF-1 were all down-regulated. The other reason might be that the balance between HIF-1 and FIH declined due to increased oxidative stress in bone marrow cavity.

The gene expression levels were studies in BMI <25 OP subgroup. Eight genes (*ADM*, *BHLHE40*, *MAP3K1*, *LOX*, *TXNIP*, *NAMPT*, *PFKFB3* and *PIM1*) were down-regulated and two genes (*ANGPTL4*, *SLC16A3*) were up-regulated in BMI <25 OP subgroup compared with control group. ADM acts as a survival factor in osteoblastic cells via a CGRP1 receptor-MEK-ERK pathway, which provides further understanding on the physiological function of ADM in osteoblasts (30). Lysyl oxidase (LOX) is a critical mediator of bone marrow cell recruitment to form the premetastatic niche (31). Thioredoxin-interacting protein (TXNIP), which is induced by oxidative stress, is a known regulator of intracellular ROS, which confirmed the relationship between ROS and OP. Nicotinamide phosphoribosyltransferase (Nampt) affects the lineage fate determination of mesenchymal stem cells (32) which could be a possible cause for decreased osteogenesis and increased adipogenesis in elder individuals. Angptl4 is up-regulated under inflammatory conditions in the bone marrow of mice (33), which might play an important role in the inflammatory condition in OP bone marrow. SLC16A3 is one of carbohydrate transporters which have not been reported concerned with OP.

Abnormal adiposity is associated with many metabolic diseases, where the link seems to be the mild and chronic inflammation occurred in obesogenic conditions. One of the mechanisms triggering inflammation has been associated with adipose tissue hypoxia (34). Studies have confirmed that hypoxia, mainly due to hypoperfusion, exists in adipose tissue no matter in obesity mice or human (15,35). Oxygen stress plays a pivotal role in normal human development and physiology, so disturbance of oxygen balance by abnormal adiposity in bone marrow may cause tissue dysfunction and affect a series of genes expression such as HIF-1α, IL-6, GLUT-1, PPAR-γ, etc., pushing the tissue toward a pro-inflammatory environment. All the above can disrupt the balanced microenvironment in bone marrow and result in BMSCs dysfunction, which may play an important role in pathophysiology of OP. Therefore, it was later investigated the influence of obesity on hypoxia pathway of BMSCs from OP patients. Hypoxia-mediated HIF-1α-activated downstream target genes were down-regulated in BMI ≥25 OP subgroup, including glycolytic enzymes (Pfkl, GYS1), carbohydrate transport and metabolism genes (*CA9*, *SLC2A1*, *SLC16A3*, *NAMPT*). AnxA2 is also expressed in cells of the osteoblast lineage and chondrocytes and may play a role in matrix mineralization (36). P4HB is involved in hydroxylation of prolyl residues in precollagen. These results demonstrated that BMI ≥25 had more negative effect on metabolic and glycolytic genes expression of BMSCs rather than VEGF which was viewed as another important downstream of HIF-1. In summary, these findings shed new light on the hypoxia pathway in OP and have implications for future researches.

Acknowledgments

Footnote

Conflicts of Interest: The authors have no conflicts of interest to declare.

Ethical Statement: This study was approved by the Ethics Committee of Shanghai Tongji Hospital (KYSB-2015-20). Informed consent was provided by all participants. The authors are accountable for all aspects of the work in ensuring that questions related to the accuracy or integrity of any part of the work are appropriately investigated and resolved.

References

1. Devlin MJ, Cloutier AM, Thomas NA, et al. Caloric restriction leads to high marrow adiposity and low bone mass in growing mice. J Bone Miner Res 2010;25:2078-88.
2. Johnson RW, Schipani E, Giaccia AJ. HIF targets in bone remodeling and metastatic disease. Pharmacol Ther

2015;150:169-77.

3. Provot S, Zinyk D, Gunes Y, et al. Hif-1alpha regulates differentiation of limb bud mesenchyme and joint development. J Cell Biol 2007;177:451-64.

4. Harrison JS, Rameshwar P, Chang V, et al. Oxygen saturation in the bone marrow of healthy volunteers. Blood 2002;99:394.

5. Spencer JA, Ferraro F, Roussakis E, et al. Direct measurement of local oxygen concentration in the bone marrow of live animals. Nature 2014;508:269-73.

6. Dong-Feng Z, Ting L, Cheng C, et al. Silencing HIF-1alpha reduces the adhesion and secretion functions of acute leukemia hBMSCs. Braz J Med Biol Res 2012;45:906-12.

7. Mohyeldin A, Garzon-Muvdi T, Quinones-Hinojosa A. Oxygen in stem cell biology: a critical component of the stem cell niche. Cell Stem Cell 2010;7:150-61.

8. Chinn IK, Blackburn CC, Manley NR, et al. Changes in primary lymphoid organs with aging. Semin Immunol 2012;24:309-20.

9. Hou R, Liu R, Niu X, et al. Biological characteristics and gene expression pattern of bone marrow mesenchymal stem cells in patients with psoriasis. Exp Dermatol 2014;23:521-3.

10. Johnson AR, Milner JJ, Makowski L. The inflammation highway: metabolism accelerates inflammatory traffic in obesity. Immunol Rev 2012;249:218-38.

11. Frommer KW, Neumann E, Lange U. Inflammation and bone: Osteoimmunological aspects. Z Rheumatol 2016;75:444-50.

12. Kuhn H, O'Donnell VB. Inflammation and immune regulation by 12/15-lipoxygenases. Prog Lipid Res 2006;45:334-56.

13. Despres JP, Arsenault BJ, Cote M, et al. Abdominal obesity: the cholesterol of the 21st century? Can J Cardiol 2008;24 Suppl D:7D-12D.

14. Hodson L. Adipose tissue oxygenation: Effects on metabolic function. Adipocyte 2014;3:75-80.

15. Hosogai N, Fukuhara A, Oshima K, et al. Adipose tissue hypoxia in obesity and its impact on adipocytokine dysregulation. Diabetes 2007;56:901-11.

16. Wellen KE, Hotamisligil GS. Obesity-induced inflammatory changes in adipose tissue. J Clin Invest 2003;112:1785-8.

17. Lee JS, Park JC, Kim TW, et al. Human bone marrow stem cells cultured under hypoxic conditions present altered characteristics and enhanced in vivo tissue regeneration. Bone 2015;78:34-45.

18. de Vries M, Hesse L, Jonker MR, et al. Pim1 kinase activity preserves airway epithelial integrity upon house dust mite exposure. Am J Physiol Lung Cell Mol Physiol 2015;309:L1344-53.

19. Jiang C, Sun J, Dai Y, et al. HIF-1A and C/EBPs transcriptionally regulate adipogenic differentiation of bone marrow-derived MSCs in hypoxia. Stem Cell Res Ther 2015;6:21.

20. Valorani MG, Montelatici E, Germani A, et al. Pre-culturing human adipose tissue mesenchymal stem cells under hypoxia increases their adipogenic and osteogenic differentiation potentials. Cell Prolif 2012;45:225-38.

21. Liu SY, He YB, Deng SY, et al. Exercise affects biological characteristics of mesenchymal stromal cells derived from bone marrow and adipose tissue. Int Orthop 2017;41:1199-209.

22. Fassio A, Idolazzi L, Rossini M, et al. The obesity paradox and osteoporosis. Eat Weight Disord 2018;23:293-302.

23. Berry DC, Jiang Y, Arpke RW, et al. Cellular Aging Contributes to Failure of Cold-Induced Beige Adipocyte Formation in Old Mice and Humans. Cell Metab 2017;25:481.

24. Lin Q, Yun Z. The Hypoxia-Inducible Factor Pathway in Adipocytes: The Role of HIF-2 in Adipose Inflammation and Hypertrophic Cardiomyopathy. Front Endocrinol (Lausanne) 2015;6:39.

25. Kim H, Koh H, Ku SY, et al. Association between polymorphisms in period genes and bone density in postmenopausal Korean women. Climacteric 2014;17:605-12.

26. Iwata T, Kawamoto T, Sasabe E, et al. Effects of overexpression of basic helix-loop-helix transcription factor Dec1 on osteogenic and adipogenic differentiation of mesenchymal stem cells. Eur J Cell Biol 2006;85:423-31.

27. Chang HC, Kao CH, Chung SY, et al. Bhlhe40 differentially regulates the function and number of peroxisomes and mitochondria in myogenic cells. Redox Biol 2019;20:321-33.

28. Cen B, Xiong Y, Song JH, et al. The Pim-1 protein kinase is an important regulator of MET receptor tyrosine kinase levels and signaling. Mol Cell Biol 2014;34:2517-32.

29. Semenza GL. Hypoxia-inducible factor 1: master regulator of O2 homeostasis. Curr Opin Genet Dev 1998;8:588-94.

30. Uzan B, Villemin A, Garel JM, et al. Adrenomedullin is anti-apoptotic in osteoblasts through CGRP1 receptors and MEK-ERK pathway. J Cell Physiol 2008;215:122-8.

31. Erler JT, Bennewith KL, Cox TR, et al. Hypoxia-induced lysyl oxidase is a critical mediator of bone marrow cell

Page 14 of 14

Zhu et al. Genes in hypoxia pathway on BMSC in OP

recruitment to form the premetastatic niche. Cancer Cell 2009;15:35-44.

32. Li Y, He X, Li Y, et al. Nicotinamide phosphoribosyltransferase (Nampt) affects the lineage fate determination of mesenchymal stem cells: a possible cause for reduced osteogenesis and increased adipogenesis in older individuals. J Bone Miner Res 2011;26:2656-64.

33. Schumacher A, Denecke B, Braunschweig T, et al. Angptl4 is upregulated under inflammatory conditions in the bone marrow of mice, expands myeloid progenitors, and accelerates reconstitution of platelets after myelosuppressive therapy. J Hematol Oncol 2015;8:64.

34. Gonzalez-Muniesa P, Quintero P, De Andres J, et al. Hypoxia: a consequence of obesity and also a tool to treat excessive weight loss. Sleep Breath 2015;19:7-8.

35. Virtanen KA, Lonnroth P, Parkkola R, et al. Glucose uptake and perfusion in subcutaneous and visceral adipose tissue during insulin stimulation in nonobese and obese humans. J Clin Endocrinol Metab 2002;87:3902-10.

36. Genetos DC, Wong A, Watari S, et al. Hypoxia increases Annexin A2 expression in osteoblastic cells via VEGF and ERK. Bone 2010;47:1013-9.

Cite this article as: Zhu Q, Shan C, Li L, Song L, Zhang K, Zhou Y. Differential expression of genes associated with hypoxia pathway on bone marrow stem cells in osteoporosis patients with different bone mass index. Ann Transl Med 2019;7(14):309. doi: 10.21037/atm.2019.06.27

Table S1 Gene data

Position	Unigene	GeneBank	Symbol	Description	Gene name
A01	Hs.441047	NM_001124	ADM	Adrenomedullin	AM
A02	Hs.167046	NM_000676	ADORA2B	Adenosine A2b receptor	ADORA2
A03	Hs.513490	NM_000034	ALDOA	Aldolase A, fructose-bisphosphate	ALDA, GSD12, MGC10942, MGC17716, MGC17767
A04	Hs.9613	NM_001039667	ANGPTL4	Angiopoietin-like 4	ANGPTL2, ARP4, FIAF, HFARP, NL2, PGAR, pp1158
A05	Hs.508154	NM_181726	ANKRD37	Ankyrin repeat domain 37	Lrp2bp, MGC111507
A06	Hs.511605	NM_004039	ANXA2	Annexin A2	ANX2, ANX2L4, CAL1H, LIP2, LPC2, LPC2D, P36, PAP-IV
A07	Hs.73722	NM_080649	APEX1	APEX nuclease (multifunctional DNA repair enzyme) 1	APE, APE1, APEN, APEX, APX, HAP1, REF1
A08	Hs.632446	NM_001668	ARNT	Aryl hydrocarbon receptor nuclear translocator	HIF-1-beta, HIF-1beta, HIF1-beta, HIF1B, HIF1BETA, TANGO, bHLHe2
A09	Hs.271791	NM_001184	ATR	Ataxia telangiectasia and Rad3 related	FRP1, MEC1, SCKL, SCKL1
A10	Hs.728782	NM_003670	BHLHE40	Basic helix-loop-helix family, member e40	BHLHB2, DEC1, FLJ99214, HLHB2, SHARP-2, STRA13, Stra14
A11	Hs.716515	NM_000057	BLM	Bloom syndrome, RecQ helicase-like	BS, MGC126616, MGC131618, MGC131620, RECQ2, RECQL2, RECQL3
A12	Hs.144873	NM_004052	BNIP3	BCL2/adenovirus E1B 19kDa interacting protein 3	NIP3
B01	Hs.131226	NM_004331	BNIP3L	BCL2/adenovirus E1B 19kDa interacting protein 3-like	BNIP3a, NIX
B02	Hs.255935	NM_001731	BTG1	B-cell translocation gene 1, anti-proliferative	–
B03	Hs.63287	NM_001216	CA9	Carbonic anhydrase IX	CAIX, MN
B04	Hs.13291	NM_004354	CCNG2	Cyclin G2	–
B05	Hs.491912	NM_006837	COPS5	COP9 constitutive photomorphogenic homolog subunit 5 (Arabidopsis)	CSN5, JAB1, MGC3149, MOV-34, SGN5
B06	Hs.517076	NM_000308	CTSA	Cathepsin A	GLB2, GSL, NGBE, PPCA, PPGB
B07	Hs.523012	NM_019058	DDIT4	DNA-damage-inducible transcript 4	Dig2, FLJ20500, REDD-1, REDD1, RP11-442H21.1, RTP801
B08	Hs.164419	NM_025219	DNAJC5	DnaJ (Hsp40) homolog, subfamily C, member 5	CSP, DKFZp434N1429, DKFZp761N1221, DNAJC5A, FLJ00118, FLJ13070
B09	Hs.511899	NM_001955	EDN1	Endothelin 1	ET1, HDLCQ7, PPET1
B10	Hs.444450	NM_022051	EGLN1	Egl nine homolog 1 (C. elegans)	C1orf12, DKFZp761F179, ECYT3, HIFPH2, HPH2, PHD2, SM20, ZMYND6
B11	Hs.515417	NM_053046	EGLN2	Egl nine homolog 2 (C. elegans)	DKFZp434E026, EIT6, FLJ95603, HIF-PH1, HIFPH1, HPH-1, HPH-3, PHD1
B12	Hs.326035	NM_001964	EGR1	Early growth response 1	AT225, G0S30, KROX-24, NGFI-A, TIS8, ZIF-268, ZNF225
C01	Hs.411641	NM_004095	EIF4EBP1	Eukaryotic translation initiation factor 4E binding protein 1	4E-BP1, 4EBP1, BP-1, MGC4316, PHAS-I
C02	Hs.517145	NM_001428	ENO1	Enolase 1, (alpha)	ENO1L1, MPB1, NNE, PPH
C03	Hs.2303	NM_000799	EPO	Erythropoietin	EP, MGC138142, MVCD2
C04	Hs.592304	NM_014584	ERO1L	ERO1-like (S. cerevisiae)	ERO1-alpha, ERO1A
C05	Hs.361463	NM_000504	F10	Coagulation factor X	FX, FXA
C06	Hs.62192	NM_001993	F3	Coagulation factor III (thromboplastin, tissue factor)	CD142, FLJ17960, TF, TFA
C07	Hs.728789	NM_005252	FOS	FBJ murine osteosarcoma viral oncogene homolog	AP-1, C-FOS
C08	Hs.436062	NM_000158	GBE1	Glucan (1,4-alpha-), branching enzyme 1	GBE
C09	Hs.466471	NM_000175	GPI	Glucose-6-phosphate isomerase	AMF, DKFZp686C13233, GNPI, NLK, PGI, PHI, SA-36, SA36
C10	Hs.386225	NM_002103	GYS1	Glycogen synthase 1 (muscle)	GSY, GYS
C11	Hs.597216	NM_001530	HIF1A	Hypoxia inducible factor 1, alpha subunit (basic helix-loop-helix transcription factor)	HIF-1alpha, HIF1, HIF1-ALPHA, MOP1, PASD8, bHLHe78
C12	Hs.500788	NM_017902	HIF1AN	Hypoxia inducible factor 1, alpha subunit inhibitor	DKFZp762F1811, FIH1, FLJ20615, FLJ22027
D01	Hs.420830	NM_152794	HIF3A	Hypoxia inducible factor 3, alpha subunit	HIF-3A, IPAS, MOP7, PASD7, bHLHe17
D02	Hs.406266	NM_000189	HK2	Hexokinase 2	DKFZp686M1669, HKII, HXK2
D03	Hs.517581	NM_002133	HMOX1	Heme oxygenase (decycling) 1	HO-1, HSP32, bK286B10
D04	Hs.116462	NM_178849	HNF4A	Hepatocyte nuclear factor 4, alpha	FLJ39654, HNF4, HNF4a7, HNF4a8, HNF4a9, HNF4alpha, MODY, MODY1, NR2A1, NR2A21, TCF, TCF14
D05	Hs.591785	NM_003897	IER3	Immediate early response 3	DIF-2, DIF2, GLY96, IEX-1, IEX-1L, IEX1, PRG1
D06	Hs.450230	NM_000598	IGFBP3	Insulin-like growth factor binding protein 3	BP-53, IBP3
D07	Hs.514505	NM_015167	JMJD6	Jumonji domain containing 6	KIAA0585, PSR, PTDSR, PTDSR1
D08	Hs.2795	NM_005566	LDHA	Lactate dehydrogenase A	GSD11, LDH1, LDHM
D09	Hs.531081	NM_002306	LGALS3	Lectin, galactoside-binding, soluble, 3	CBP35, GAL3, GALBP, GALIG, L31, LGALS2, MAC2
D10	Hs.102267	NM_002317	LOX	Lysyl oxidase	MGC105112
D11	Hs.657756	NM_005921	MAP3K1	Mitogen-activated protein kinase kinase kinase 1	MAPKKK1, MEKK, MEKK1
D12	Hs.132966	NM_000245	MET	Met proto-oncogene (hepatocyte growth factor receptor)	AUTS9, HGFR, RCCP2, c-Met
E01	Hs.407995	NM_002415	MIF	Macrophage migration inhibitory factor (glycosylation-inhibiting factor)	GIF, GLIF, MMIF
E02	Hs.297413	NM_004994	MMP9	Matrix metallopeptidase 9 (gelatinase B, 92kDa gelatinase, 92kDa type IV collagenase)	CLG4B, GELB, MANDP2, MMP-9
E03	Hs.501023	NM_005962	MXI1	MAX interactor 1	MAD2, MGC43220, MXD2, MXI, bHLHc11
E04	Hs.489615	NM_005746	NAMPT	Nicotinamide phosphoribosyltransferase	1110035O14Rik, DKFZp666B131, MGC117256, PBEF, PBEF1, VF, VISFATIN
E05	Hs.596314	NM_003743	NCOA1	Nuclear receptor coactivator 1	F-SRC-1, KAT13A, MGC129719, MGC129720, RIP160, SRC1, bHLHe42, bHLHe74
E06	Hs.372914	NM_006096	NDRG1	N-myc downstream regulated 1	CAP43, CMT4D, DRG1, GC4, HMSNL, NDR1, NMSL, PROXY1, RIT42, RTP, TARG1, TDD5
E07	Hs.654408	NM_003998	NFKB1	Nuclear factor of kappa light polypeptide gene enhancer in B-cells 1	DKFZp686C01211, EBP-1, KBF1, MGC54151, NF-kappa-B, NF-kappaB, NFKB-p105, NFKB-p50, NFkappaB, p105, p50
E08	Hs.707978	NM_000603	NOS3	Nitric oxide synthase 3 (endothelial cell)	ECNOS, eNOS
E09	Hs.467701	NM_002539	ODC1	Ornithine decarboxylase 1	ODC
E10	Hs.500047	NM_000917	P4HA1	Prolyl 4-hydroxylase, alpha polypeptide I	P4HA
E11	Hs.464336	NM_000918	P4HB	Prolyl 4-hydroxylase, beta polypeptide	DSI, ERBA2L, GIT, P4Hbeta, PDI, PDIA1, PHDB, PO4DB, PO4HB, PROHB
E12	Hs.470633	NM_002610	PDK1	Pyruvate dehydrogenase kinase, isozyme 1	–
F01	Hs.445534	NM_002616	PER1	Period homolog 1 (Drosophila)	MGC88021, PER, RIGUI, hPER
F02	Hs.195471	NM_004566	PFKFB3	6-phosphofructo-2-kinase/fructose-2,6-biphosphatase 3	FLJ37326, IPFK2, PFK2
F03	Hs.476217	NM_004567	PFKFB4	6-phosphofructo-2-kinase/fructose-2,6-biphosphatase 4	–
F04	Hs.255093	NM_002626	PFKL	Phosphofructokinase, liver	DKFZp686G1648, DKFZp686L2097, FLJ30173, FLJ40909, PFK-B
F05	Hs.26010	NM_002627	PFKP	Phosphofructokinase, platelet	FLJ40226, FLJ44165, PFK-C, PFKF
F06	Hs.592599	NM_002629	PGAM1	Phosphoglycerate mutase 1 (brain)	PGAM-B, PGAMA
F07	Hs.252820	NM_002632	PGF	Placental growth factor	D12S1900, PGFL, PLGF, PlGF-2, SHGC-10760
F08	Hs.78771	NM_000291	PGK1	Phosphoglycerate kinase 1	MGC117307, MGC142128, MGC8947, MIG10, PGKA
F09	Hs.81170	NM_002648	PIM1	Pim-1 oncogene	PIM
F10	Hs.534770	NM_002654	PKM2	Pyruvate kinase, muscle	CTHBP, MGC3932, OIP3, PK3, PKM, TCB, THBP1
F11	Hs.77274	NM_002658	PLAU	Plasminogen activator, urokinase	ATF, UPA, URK, u-PA
F12	Hs.479396	NM_005349	RBPJ	Recombination signal binding protein for immunoglobulin kappa J region	CBF1, IGKJRB, IGKJRB1, KBF2, MGC61669, RBP-J, RBPJK, RBPSUH, SUH, csl
G01	Hs.515846	NM_006666	RUVBL2	RuvB-like 2 (E. coli)	ECP51, INO80J, REPTIN, RVB2, TIH2, TIP48, TIP49B
G02	Hs.414795	NM_000602	SERPINE1	Serpin peptidase inhibitor, clade E (nexin, plasminogen activator inhibitor type 1), member 1	PAI, PAI-1, PAI1, PLANH1
G03	Hs.500761	NM_004207	SLC16A3	Solute carrier family 16, member 3 (monocarboxylic acid transporter 4)	MCT 3, MCT 4, MCT-3, MCT-4, MCT3, MCT4, MGC138472, MGC138474
G04	Hs.473721	NM_006516	SLC2A1	Solute carrier family 2 (facilitated glucose transporter), member 1	DYT17, DYT18, GLUT, GLUT1, GLUT1DS, MGC141895, MGC141896, PED
G05	Hs.419240	NM_006931	SLC2A3	Solute carrier family 2 (facilitated glucose transporter), member 3	FLJ90380, GLUT3
G06	Hs.529618	NM_003234	TFRC	Transferrin receptor (p90, CD71)	CD71, TFR, TFR1, TRFR
G07	Hs.654481	NM_000546	TP53	Tumor protein p53	FLJ92943, LFS1, P53, TRP53
G08	Hs.524219	NM_000365	TPI1	Triosephosphate isomerase 1	MGC88108, TIM, TPI
G09	Hs.533977	NM_006472	TXNIP	Thioredoxin interacting protein	EST01027, HHCPA78, THIF, VDUP1
G10	Hs.454534	NM_003367	USF2	Upstream transcription factor 2, c-fos interacting	FIP, bHLHb12
G11	Hs.519320	NM_003374	VDAC1	Voltage-dependent anion channel 1	MGC111064, PORIN, VDAC-1
G12	Hs.73793	NM_003376	VEGFA	Vascular endothelial growth factor A	MGC70609, MVCD1, VEGF, VPF
H01	Hs.520640	NM_001101	ACTB	Actin, beta	PS1TP5BP1
H02	Hs.534255	NM_004048	B2M	Beta-2-microglobulin	–
H03	Hs.592355	NM_002046	GAPDH	Glyceraldehyde-3-phosphate dehydrogenase	G3PD, GAPD, MGC88685
H04	Hs.412707	NM_000194	HPRT1	Hypoxanthine phosphoribosyltransferase 1	HGPRT, HPRT
H05	Hs.546285	NM_001002	RPLP0	Ribosomal protein, large, P0	L10E, LP0, MGC111226, MGC88175, P0, PRLP0, RPP0
H06	N/A	SA_00105	HGDC	Human genomic DNA contamination	HIGX1A
H07	N/A	SA_00104	RTC	Reverse transcription control	RTC
H08	N/A	SA_00104	RTC	Reverse transcription control	RTC
H09	N/A	SA_00104	RTC	Reverse transcription control	RTC
H10	N/A	SA_00103	PPC	Positive PCR control	PPC
H11	N/A	SA_00103	PPC	Positive PCR control	PPC
H12	N/A	SA_00103	PPC	Positive PCR control	PPC